Supporting Information

Growth and characterization of the all-inorganic lead halide perovskite semiconductor $CsPbBr_3$ single crystals

Mingzhi Zhang [a], Zhiping Zheng *, [a], Qiuyun Fu [a, b], Zhen Chen [a], Jianle He [a], Sen Zhang [a], Liang Yan, Yunxiang Hu [a], Wei Luo [a]

[a] School of Optical and Electronic Information, Huazhong University of Science and Technology, Wuhan 430074, PR China

[b] State Key Laboratory of Material Processing and Die & Mold Technology, Huazhong University of Science and Technology, Wuhan 430074, PR China

Full affiliation address: No.1037, Luoyu Road, Hongshan District, Wuhan, Hubei Province, China, 430074

Corresponding author：Zhiping Zheng

Email：zzp@mail.hust.edu.cn

Contents

I. Experimental details

1.1 Thermodynamics characterization

The thermogravimetric and differential scanning calorimetry analysis (TGA-DSC) of the $CsPbBr_3$ powders was carried out using a NETZSCH Instrument STA449F3 by holding 7.72 mg of $CsPbBr_3$ in an Al_2O_3 crucible at N_2 atmosphere with measurement temperature range of 40 °C - 570 °C. The heating rate of 10 °C min^{-1} from 40 °C to 570 °C min^{-1} and cooling rate of 10 °C min^{-1} from 570 °C to 450°C were set in advance. The TGA-DSC curves of $CsPbBr_3$ were shown in Figure S1. An endothermic peak at 567 °C and an exothermic peak at 550 °C can be observed, which corresponded to the melting and solidifying point of $CsPbBr_3$, respectively. In order to investigate the effect of environment on thermodynamics characterization, other TGA-DSC analysis results were conducted under different conditions. The TGA-DSC curves were shown in Figure S2.

1.2 A tube furnace and EDG crystal growth

The growth of single crystal was conducted in a self-designed vertical two-zone tube furnace by a simplified electronic dynamic gradient (EDG) method. A simple schematic diagram of the furnace was shown in Figure S3(a). The furnace was consisted of three parts: a heating module, an adiabatic module and a temperature control module. The average temperature gradient in the growth zone where the melt located (marked as 5) could be tuned from 5 to 15 °C/cm. Figure S3(b) showed the temperature profile with a temperature gradient of 10 °C/cm. The dotted lines of 567°C and 550°C are two isothermal lines, representing melting and solidifying points of the powders, respectively.

The procedure of $CsPbBr_3$ crystal growth is described as follows. A certain amount of $CsPbBr_3$ polycrystalline powders was loaded in a high-purity quartz ampule which had a conical tip, and then the quartz ampule was sealed under a 0.1 Pa pressure. The tube furnace was first heated up to the melting point of $CsPbBr_3$ polycrystalline powders and held for a few hours. Then the tube furnace was cooled for crystal growth. The cooling rate during the crystal growth process was rigorously controlled at 0.5 °C/h. As $CsPbBr_3$ has a phase-transition temperature of 130 °C, crystal growth process was followed by a special cooling process at three steps. At first step, the cooling process was conducted at a cooling rate of 10 °C/h until the minimum temperature of the ingots reached 130 °C. At second step, the cooling process

proceeded at a smaller cooling rate of 1 °C/h until the temperature of the whole ingot was below 130 °C. At third step, the temperature of the furnace decreased to room temperature in few hours to finish the crystal growth of $CsPbBr_3$.

1.3 Temperature-dependent XRD characterization

The phase transitions of $CsPbBr_3$ were studied using the temperature-dependent X-ray powder diffraction, where the crystal structure of $CsPbBr_3$ had changed with the temperature increasing from room temperature (300 K) to high temperature (500 K). The temperature-dependent XRD of $CsPbBr_3$ was shown in Figure S5, with a zoom-in to an area of interest between 14° to 35°. The magnification of the 14°-35° region of the XRD pattern indicated the cubic-to-tetragonal and tetragonal-to-orthorhombic phase transitions. The two phase transitions which occurred at around 360 K and 400 K can be deduced from the enlarged pattern. When the temperature went up to 410 K, the disappearance of the splitting diffraction peaks at 15.198°, 30.633° could be observed clearly in Figure S5. And the weak diffraction peaks at 24.165°, 28.587° disappeared when the temperature went up to 370 K could be also observed clearly in Figure S5.

1.4 Crystal cutting and sample preparation

The as-grown crystal had a size of 60 mm in length. The conical part of the crystal ingot was about 30 mm in length as shaped by the ampule, and it was irregular with a gradually varied diameter. The middle isometric part of the crystal was chosen for investigation. Figure S6 showed a photograph of isometric part of the as-grown $CsPbBr_3$ crystal and the cutting schematic diagram. A hacksaw equipped with diamond was used to cut the crystal. To remove the physical damage and flatten the wafer surface, cutting was followed by careful surface treatments. Al_2O_3 abrasives with 14 μm in diameter and then 7, 1.5 and 0.5 μm were used to polish the surfaces of the wafers in turns. Then the polished wafers were immersed in a concentration of 5% bromine methanol solution for 30 s to remove the physical damage of the surface caused by the cutting and mechanical polishing processes.

II. Supporting Figures

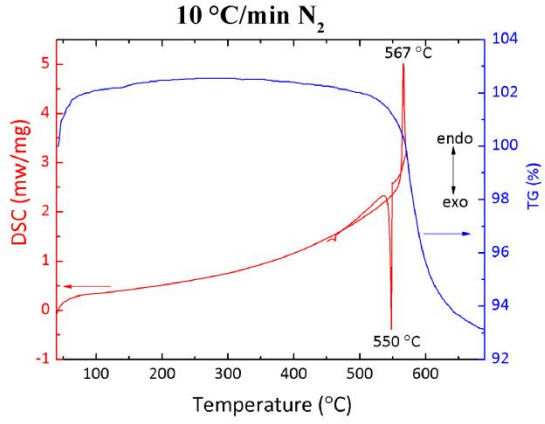

Figure S1 TGA-DSC curves of $CsPbBr_3$ powders measured at N_2 atmosphere with a cooling rate of 10 °C/ min

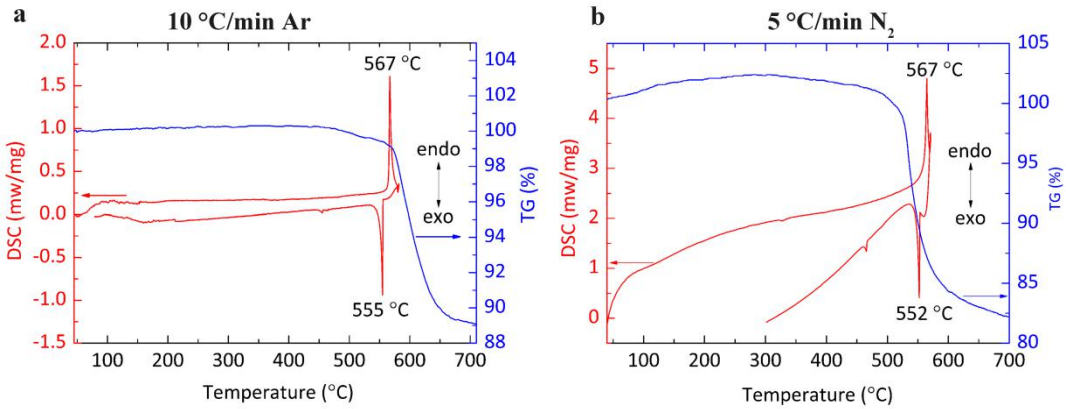

Figure S2 TGA-DSC curves of $CsPbBr_3$ powders measured at different conditions (a) Ar atmosphere with a cooling rate of 10 °C/ min; (b) N_2 atmosphere with a cooling rate of 5 °C/ min

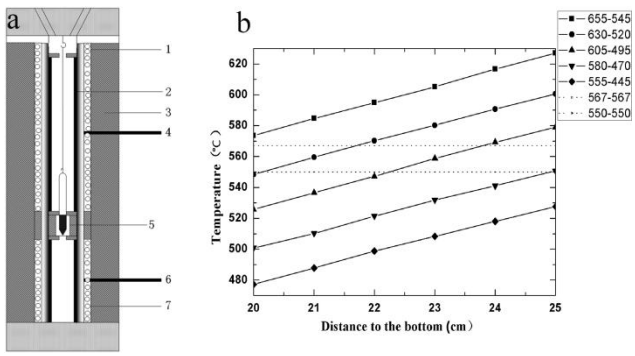

Figure S3 Schematic diagram (a) and the temperature profile (b) of the tube furnace

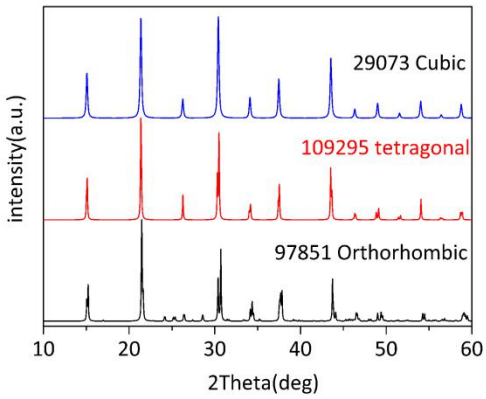

Figure S4 Standard patterns of orthorhombic, tetragonal and cubic phase from the ICSD database

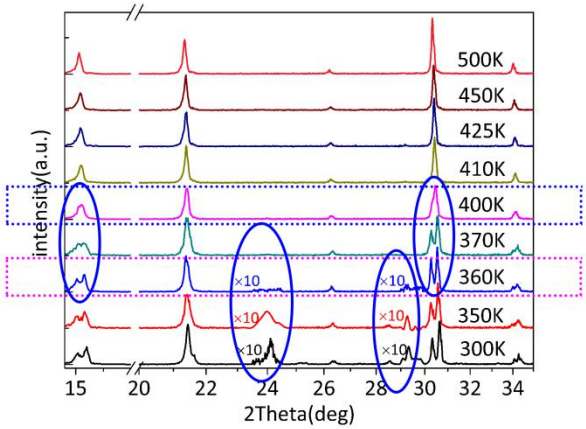

Figure S5 The temperature-dependent XRD of $CsPbBr_3$, with a zoom-in to an area of interest of 14° to 35°

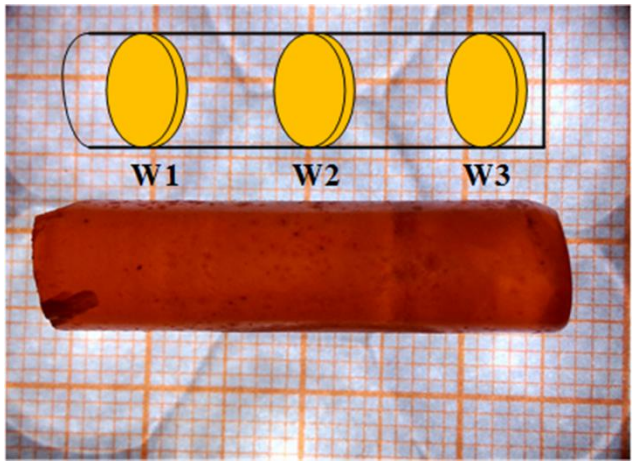

Figure S6 Photograph of isometric part of the crystal and the cutting schematic diagram

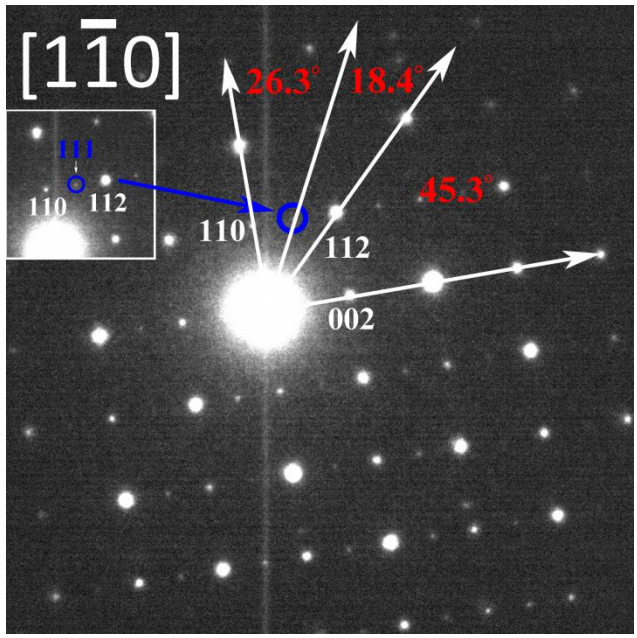

Figure S7 The angles among the neighbor diffraction spots

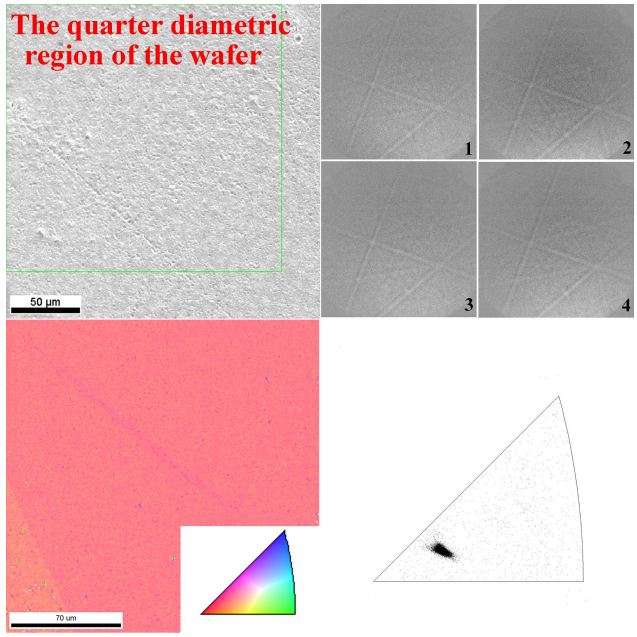

Figure S8 EBSD orientation map in the quarter diametric region of the $CsPbBr_3$ wafer

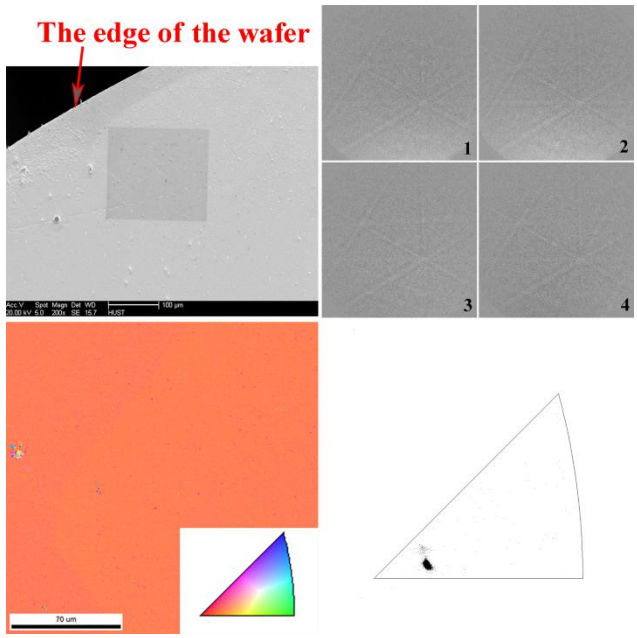

Figure S9 EBSD orientation map at the edge region of the $CsPbBr_3$ wafer